Characterization of the wind field in the Kuroshio extended body sea based on buoy observation

Ming Ke [1, *] and Boyuan Wang [2]

[1] School of Marine and Atmospheric Sciences, Ocean University of China, Qingdao, China

[2] ChongBen Honors College, Ocean University of China, Qingdao, China

* Corresponding Author Email: keming@stu.ouc.edu.cn

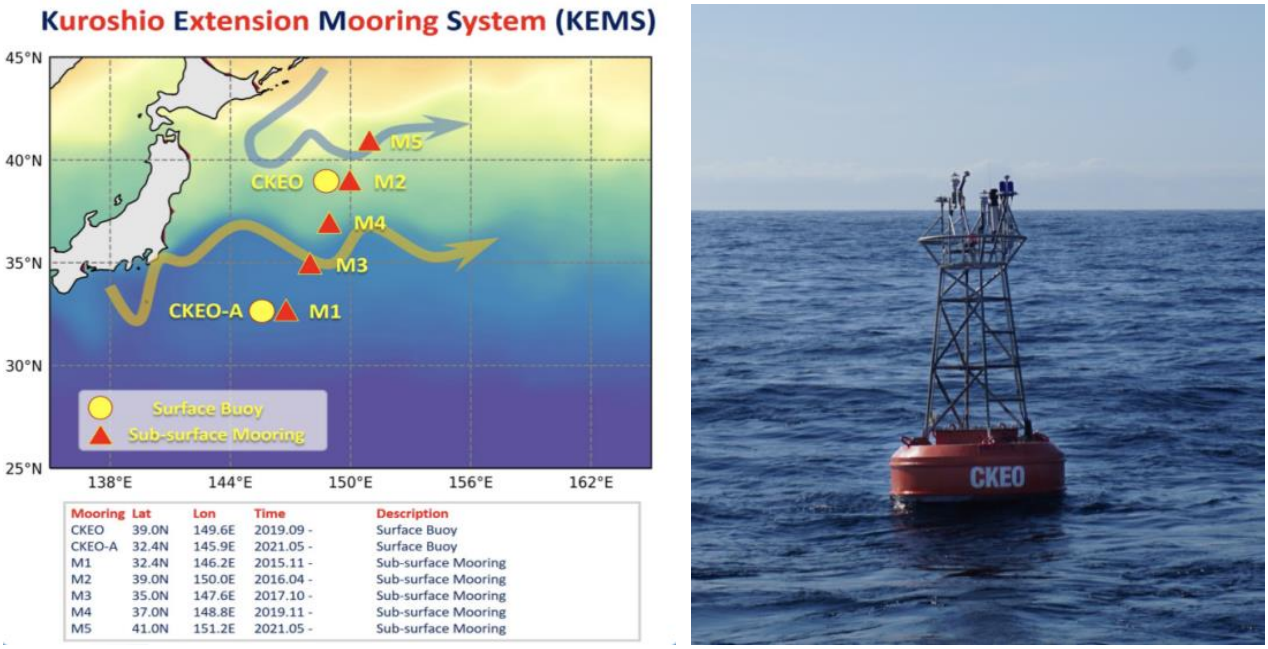
Abstract. In this paper, we propose to combine the data from CKEO and KEO buoys and reanalysis data to study the prevailing wind types, temperature changes and carbon fluxes in the Kuroshio Extension in different seasons in recent years, in order to deepen our understanding of the physical and chemical environment and its evolution in the sea. In this paper, we analyze the characteristics of the wind field of the Kuroshio Extension using the CKEO buoy system at a fixed coordinate (149.25°E, 39°N) in the northwest Pacific Ocean, using four methods: wind speed and direction rose diagram, wind speed comparison line diagram, temperature comparison line diagram and carbon flux variation line diagram. Compared with the KEO buoy observation system, the CKEO buoy observation system provides high quality sea-air observation data in the Kuroshio Extension, which provides valuable information for the study of sea-air interaction in the Kuroshio Extension.

Keywords: Buoy observation; wind field characteristics; wind speed and direction rose diagram; wind speed comparison line graph.

1. Introduction

The Kuroshio Extension Area (KEA) in the northwest Pacific Ocean is one of the most active areas of global oceanic and atmospheric multi-scale dynamical processes, and is also a "hot spot" area of biogeochemical cycles, whose changes have an important influence on the climate change in China [1]. However, due to the influence of strong storms, strong currents and other harsh environments, it is difficult to observe this area, and it has been a "desert area" for long-term continuous ocean observation data. Until 2014, only one set of large buoy observation system from the United States was maintained in this area for a long time, but in the same year, the Ocean Pilot National Laboratory and China Ocean University also started the journey of deep and distant sea observation, and successfully deployed China's first 6000m class deep sea submersible system in this area in November 2015, and successfully recovered it in April 2016. In the following three years, researchers from the Ocean Pilot National Laboratory and the Ocean University of China continuously optimized the structural design of the submersible system, broke through the bottleneck of real-time underwater data transmission technology such as inductive coupling transmission at large depths, and realized the stable and reliable transmission of deep-sea data in this sea area for the first time in the international arena [2]. The system is suitable for high sea state conditions in the mid-latitude sea area, and can meet the continuous and stable normal operation in the harsh working environment, which lays the technical foundation for long-term fixed-point continuous and reliable observation of core parameters at the sea-gas interface at key stations.

The global carbon cycle is an important process affecting the Earth's climate system, and the sea-air CO2 flux is a critical part of it, which is very important for the proposed and understanding of the coupling and changes of the ocean-atmosphere system [3].



Mooring	Lat	Lon	Time	Description
CKEO	39.0N	149.6E	2019.09 -	Surface Buoy
CKEO-A	32.4N	145.9E	2021.05 -	Surface Buoy
M1	32.4N	146.2E	2015.11 -	Sub-surface Mooring
M2	39.0N	150.0E	2016.04 -	Sub-surface Mooring
M3	35.0N	147.6E	2017.10 -	Sub-surface Mooring
M4	37.0N	148.8E	2019.11 -	Sub-surface Mooring
M5	41.0N	151.2E	2021.05 -	Sub-surface Mooring

Fig 1. Real-time observation system of Kuroshio extension and CKEO buoy diagram.

2. Introduction to data and methods

2.1. Wind speed and direction rose chart

The data were collected by the CKEO buoy system for the wind field at a fixed coordinate (149.25°E, 39°N) in the Kuroshio Extension in the Northwest Pacific Ocean. 2019-2020 data were collected by the CKEO-01 buoy, 2020-2021 data were collected by the CKEO-02 buoy, and 2021-2022 data for the first half of the year were collected by the CKEO-03 buoy. Buoy.

Based on the wind field data obtained from 2019-10-1 to 2022-3-25, the measurement periods were set to one month and one week, respectively, and the percentages of each wind direction and wind speed were averaged and the wind speed and wind direction rose diagrams were drawn at a certain scale. The wind direction indicated on the rose diagram is the direction from the outside to the center of the area; the line segments drawn in each direction according to the statistical values indicate the size of the wind frequency in this direction, and the longer the line segment, the more times the wind direction appears. The line segments indicating the wind frequency in each direction are drawn in different colors according to the percentage of wind speed values, that is, the average wind speed in each wind direction is indicated.

2.2. Wind Speed Comparison Line Chart

The wind speed data provided by the CKEO buoy from 2022.6.22-2022.11.4 were compared with the KEO buoy data of the same period and the correlation coefficient was calculated.

$$r(X,Y) = \frac{Cov(X,Y)}{\sqrt{Var[X]\,Var[Y]}} \tag{1}$$

Where Cov(X, Y) is the covariance of X and Y, Var[X] is the variance of X, and Var[Y] is the variance of Y. The closer the correlation coefficient is to 1, the greater the correlation is.

2.3. Temperature Comparison Line Chart

The atmospheric temperature data provided by the CKEO buoy from 2022.6.22-2022.11.4 were compared with the KEO buoy data of the same period and the correlation coefficients were calculated.

2.4. Carbon flux change line graph

The global carbon cycle is an important process affecting the Earth's climate system, and the sea-air CO2 flux is a critical part of it, which is important for modeling and understanding the coupling and changes of the ocean-atmosphere system.

Most current estimates of CO2 fluxes at the sea-gas interface are based on the following block equation:

$$F = k_W \cdot s \cdot (p_{CO_{2W}} - p_{CO_{2A}}) \tag{2}$$

Where F is the CO2 gas flux; is the gas exchange rate; s is the solubility (as a function of temperature and salinity); pCO2W and pCO2A represent the partial pressure of CO2 in seawater and atmosphere, respectively. Where CO2 transport from seawater to air is in the positive direction.

The most critical aspect in the use of the bulk equation is the estimation of the gas exchange rate kW. The estimation about kW is usually parameterized empirically based on the observed data using the wind speed polynomial with the following equation.

$$k_W = (Sc / Scr)^{-\frac{1}{2}}(a + bU + cU^2 + dU^3) \tag{3}$$

Sc is the Schmidt number, defined as the ratio of the viscosity coefficient of seawater motion to the molecular diffusion coefficient of the measured gas, which is related to the seawater temperature; Scr is the Schmidt number corresponding to a water temperature of 20°C.

$$Sc = \frac{\nu}{D} \tag{4}$$

$$\nu = \frac{0.01775}{1 + 0.0337t + 0.000221t^2} \tag{5}$$

The seawater kinematic viscosity coefficient is considered to be temperature dependent only and is calculated as Eq. (4). In calculations where accuracy is not required, the CO2 molecular diffusion coefficient DCO2 is approximated to be 20 times that of O2 with a value of 2.6 × 10-4m2s-1.

The kW fitting equation chosen for this paper is the gas exchange rate equation given by Wanninkhof using the latest 14C results, and the equation is as follows:

$$k_W = 0.251U_{10}^2(Sc / 660)^{-\frac{1}{2}} \tag{6}$$

Where, U10 is the wind speed at 10m height.

For the calculation of carbon dioxide solubility s in seawater, it is calculated according to the solubility equation of Weiss (1974):

$$\ln s = A_1 + A_2(100 / T) + A_3 \ln(T / 100) + S[B_1 + B_2(T / 100) + B_3(T / 100)^2] \tag{7}$$

Where T is the sea surface temperature, S is the practical salinity, and the data come from buoy observations. A1, A2, A3, B1, B2, and B3 look up the table to get the data. The unit of solubility s is mol/kg.

The partial pressure of carbon dioxide in the buoy and the calculated kW and s data are substituted into equation Eq. (1) to find the carbon dioxide flux in the study area.

3. Analysis of results

3.1. Wind speed and direction rose chart

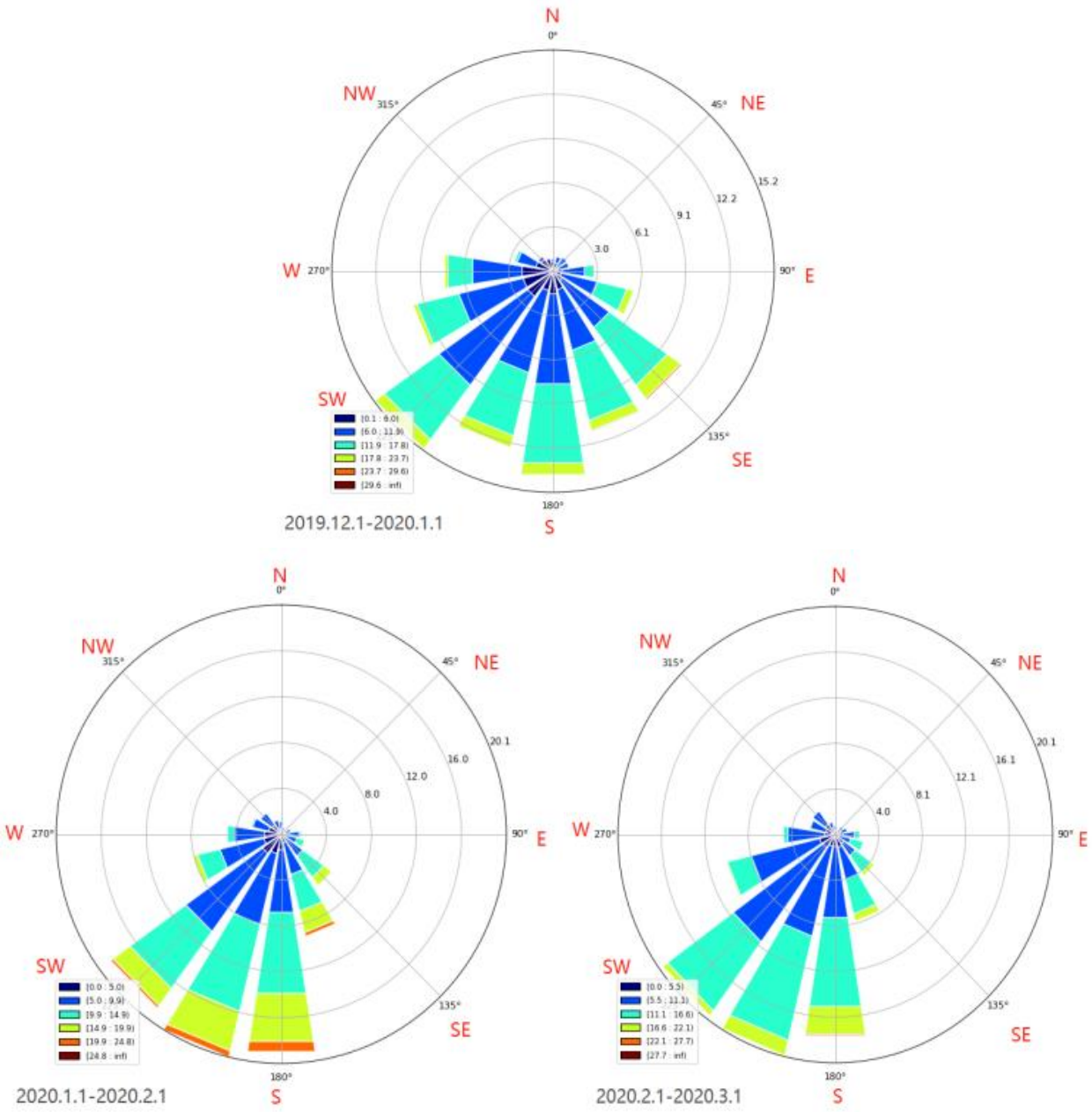


Fig 2. Rosette of wind speed and direction in 8 directions from 2019.12.1 to 2020.3.1.

From the statistical results of the 8-directional wind speed and wind direction rose diagram from 2019.12.1-2020.3.1 in terms of months, it can be concluded that before March 2020, the main wind direction at the buoy placement site is southwest wind, and the wind speed size is mostly concentrated in 5.0m/s~16.6m/s, and the wind speed has a tendency to increase with the passage of time, and the wind direction gradually moves southward.

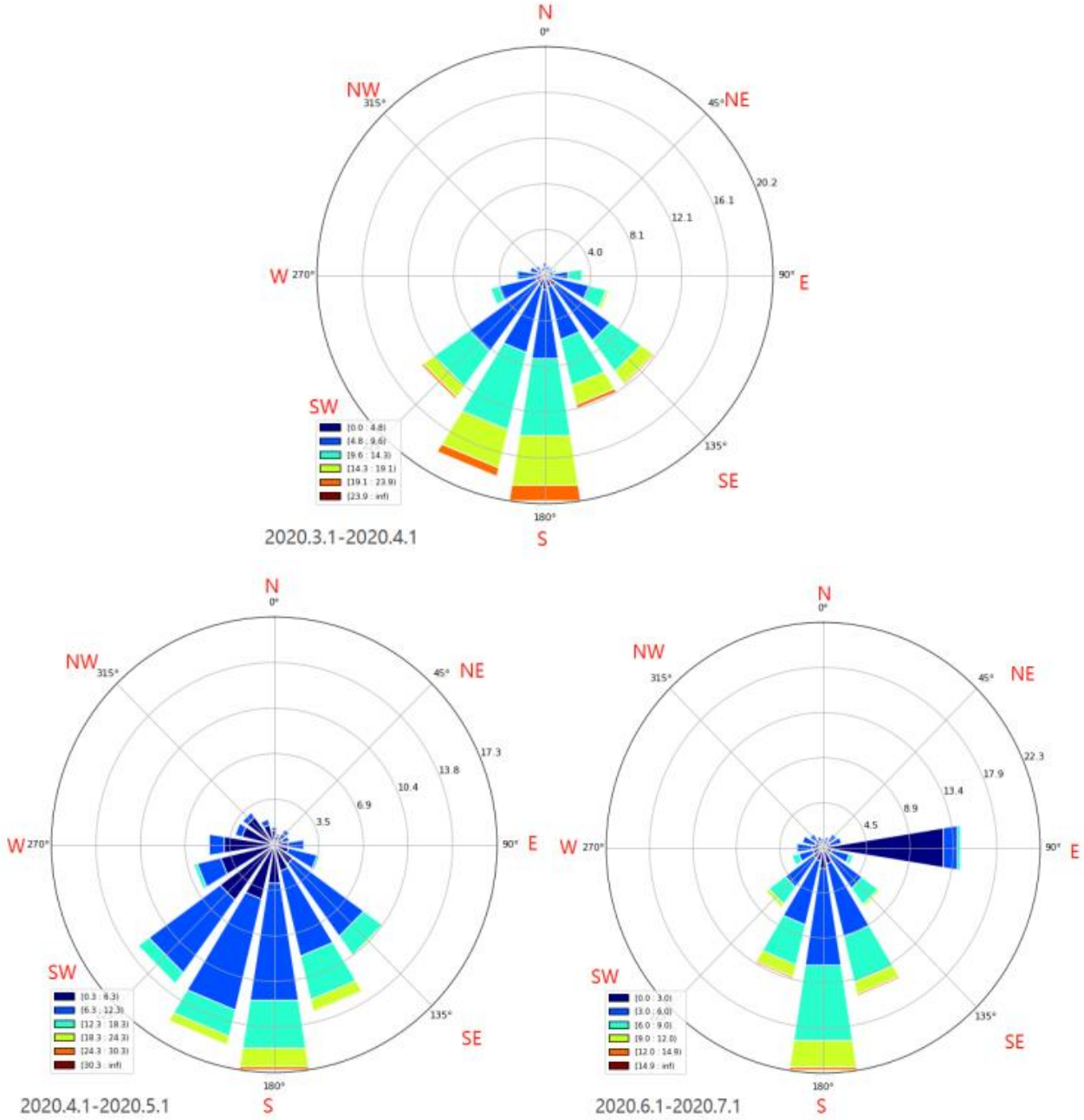


Fig 3. Rosette of wind speed and direction in 8 directions from 2020.3.1 to 2020.7.1.

From the statistical results of the 8-directional wind speed and wind direction rose diagrams from 2020.3.1 to 2020.7.1 on a monthly basis, it can be concluded that: during this time interval, the main wind direction at the buoy placement site is due south, and the wind speed size is mostly concentrated in 3.0m/s~11.6m/s, and with the passage of time, the wind speed first increases and then decreases, and the wind direction gradually moves to the east, even in June, there has been accounted for about 13.4% of the wind direction due east, the wind speed is small, mainly concentrated in 3.0m/s or less.

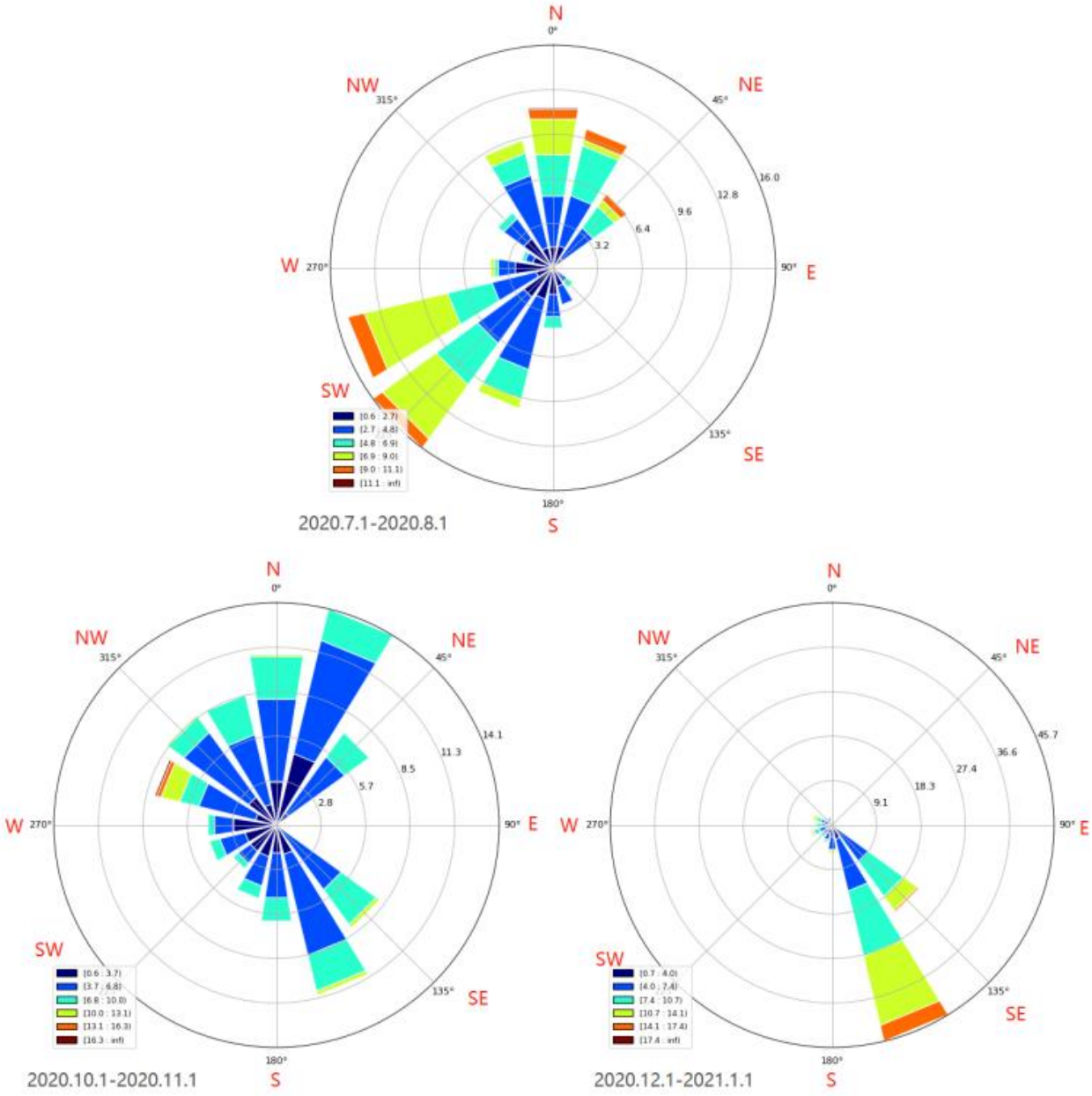


Fig 4. Rosette of wind speed and direction in 8 directions from 2020.7.1 to 2021.1.1.

From the statistical results of the 8-directional wind speed and wind direction rose diagram from 2020.7.1 to 2021.1.1 on a monthly basis, it can be concluded that the wind direction at the buoy placement site varied greatly during this time interval, and the wind direction in the first four months was mainly southwesterly, the distribution of wind direction was more dispersed, and the wind speed size was mainly concentrated in 3.0m/s~11.6m/s, and the wind direction in the last two months was more concentrated, mainly southeasterly winds to the south, the wind speed size is more evenly distributed in all directions, and the wind speed has a tendency to increase with the passage of time.

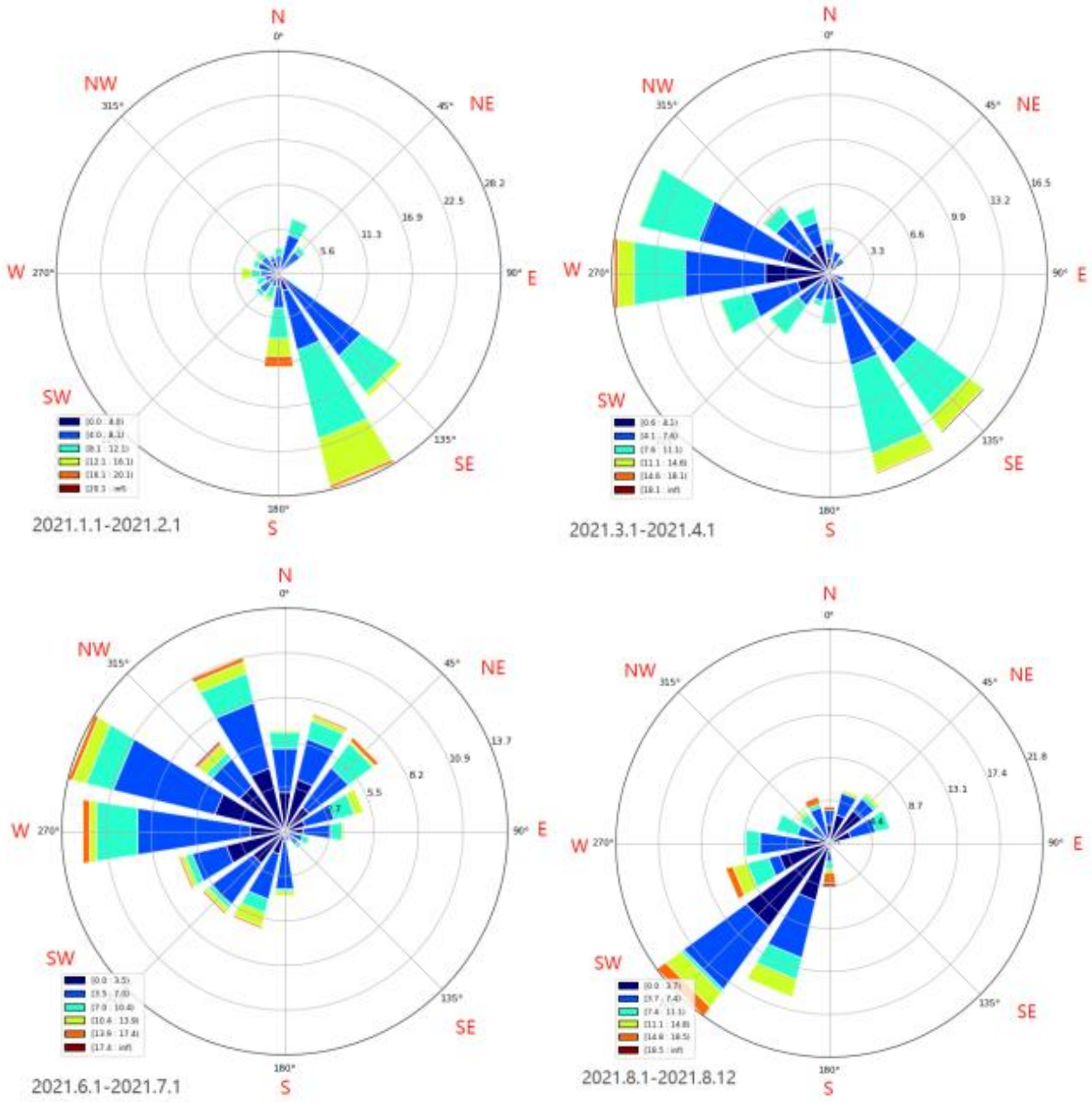


Fig 5. Rosette of wind speed and direction in 8 directions from 2021.1.1 to 2021.8.12.

From 2021.1.1-2021.8.12, the statistical results of the 8 directional wind speed and wind direction rosettes in monthly units can be concluded: during this time interval, the wind direction at the buoy placement site varied greatly, the wind direction was more concentrated in the first two months, and the main wind direction was still south-southeast, and the distribution of wind direction was more dispersed in the last 6 months, and the overall wind speed decreased and then increased with the passage of time.

In the time period of 2021.8.12-2021.11.27 the buoys were recovered, so there is no relevant data.

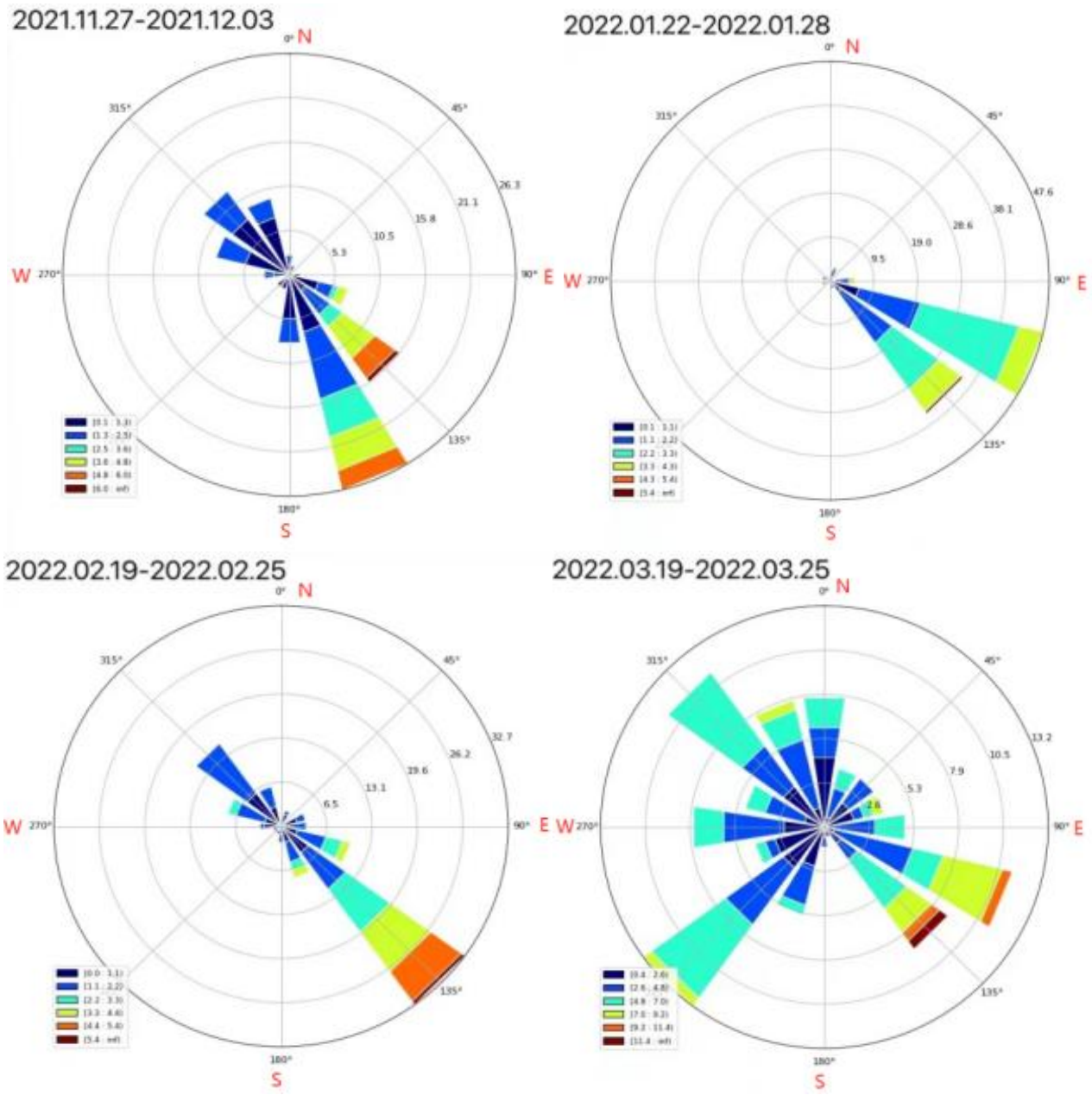
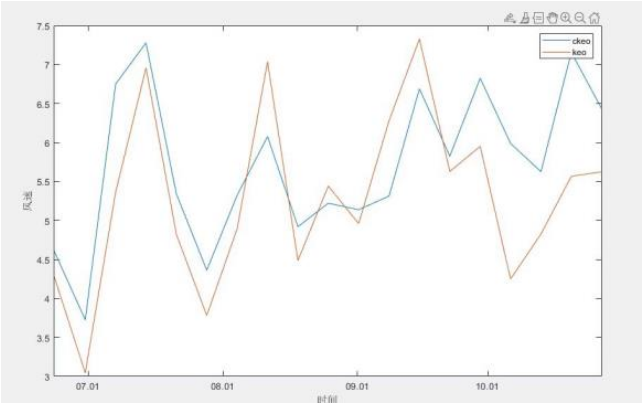
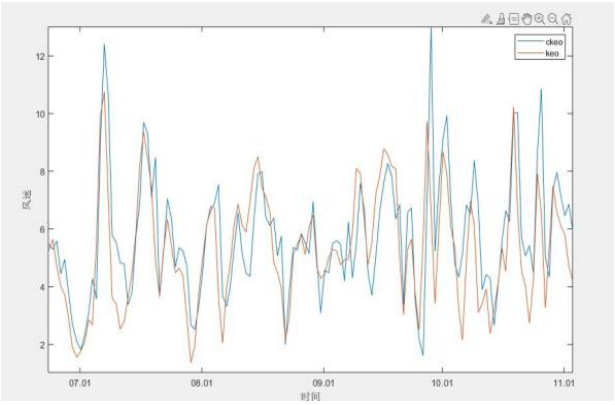


Fig 6. Rosette of wind speed and direction in 8 directions from 2021.12.3 to 2022.3.25.

In this period of time interval, the first few months the wind direction is more concentrated, the main wind direction is east-southeast, the wind speed size is concentrated in 0.9m/s ~ 5.4m/s, the wind direction gradually moved north; the last month has appeared higher wind speed, accounting for a relatively large northwest wind.

3.2. Wind Speed Comparison Line Chart



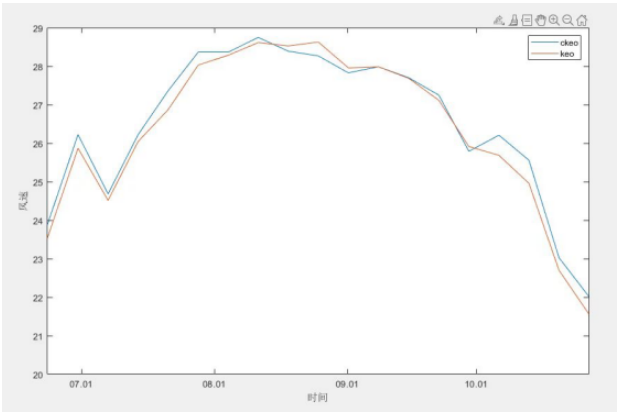


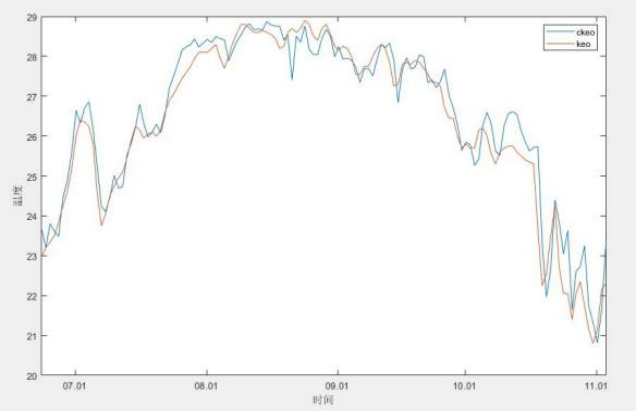
Correlation value: 0.7119 Correlation value: 0.7320

Fig 7. Wind Speed Comparison Line Chart.

From 2022.6.22 to 2022.7.4 CKEO buoy and KEO buoy wind speed comparison line graphs, we can see that the data trends of both are generally consistent and correlated; the comparison of the two graphs shows that the correlation is higher when the graphs are made on a daily basis than when the graphs are made by taking the average of each week's data.

3.3. Temperature Comparison Line Chart





Correlation value: 0.9420 Correlation value: 0.9681

Fig 8. Temperature Comparison Line Chart.

From 2022.6.22 to 2022.7.4 CKEO buoy and KEO buoy temperature comparison line graphs, it can be seen that the data trends of both are generally consistent and much correlated; the comparison of the two graphs shows that the correlation is higher when plotted on a daily basis than when plotted by taking each week's data as an average.

3.4. Carbon flux comparison line graph

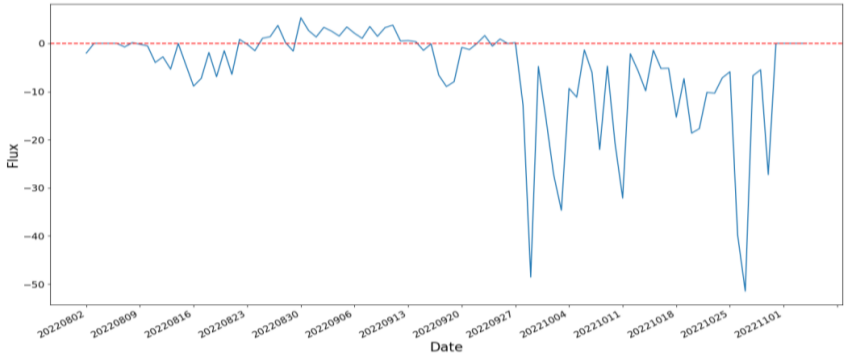


Fig 9. Carbon flux comparison line graph.

4. Summary

Compared with the KEO buoy observation system, the CKEO buoy observation system provides high quality sea-air observations in the Kuroshio extended body region, which provides valuable measured data for studying sea-air interactions in the Kuroshio extended body region and produces a series of academic research results, which are widely used in numerical weather forecasting, data reanalysis, satellite data calibration and other fields [4]. From the perspective of material exchange, the Kuroshio Extension is a hot sea area for sea-air material exchange, which plays an important role in global climate change and is an important reservoir of atmospheric CO2.

The successful construction of the real-time observation system of the Kuroshio Extension in the Northwest Pacific Ocean provides a long-term, continuous and integrated observation platform to elucidate the multi-scale energy transfer and sea-air interaction processes in the ocean, and to reveal the coupling mechanism of multi-scale physical-chemical-biological processes. In the future, the system will be continuously updated and improved, and the data will be openly shared globally to provide continuous observational data support for in-depth research on ocean and climate change, ocean carbon cycle, and sustainable development and utilization of marine biological resources.

Marine carbon sink and marine environment are directly or indirectly affected by human activities. Therefore, at the national level, it is important to further clarify the policies of marine ecosystem protection, restoration and management, as well as to control the amount of marine carbon sinks, in order to restore and develop the habitat base of marine carbon sinks and mitigate ocean acidification. The integration of marine carbon sinks into the protective policy framework of management departments and annual government plans, social, economic and biological assessment of marine ecosystems, further regulation of various marine exploitation activities, strengthening control of overfishing and marine pollution, and protection of marine environment and biodiversity, so as to better utilize the effectiveness of the solubility pump, biological pump and micro-biological pump. The reasons for the increase of CO2 emissions in different regions are considered comprehensively, and national marine carbon sink plans or policies are formulated or revised to improve integrated coastal zone management and marine spatial planning [5].

References

[1] Xing Xiaobo. Study on the spatial and temporal variability of the vertical thermal structure of the three-dimensional temperature field of the Kuroshio extension [D]. Institute of Oceanography, Chinese Academy of Sciences. University of Chinese Academy of Sciences, 2020.

[2] Transparent Ocean Project: The first phase of the real-time observation system of the Kuroshio Current Extended Body in the Northwest Pacific Ocean is completed. Ocean National Laboratory,2020

[3] Yan Junyue, Liu Jiumeng, Jiang Guorong et al. Progress of sea-air flux exchange in the South China Sea[J]. Advances in Earth Science, 2007, 22(7): 685-697.

[4] CHEN Zhaohui, LIN Xiaopei, MA Xin, GUAN Yanfeng, ZHOU Chun, ZHANG Yueqi, MARK. A review and outlook of Kuroshio extensions in the Northwest Pacific[J]. Geological foreground, 2022, 29(5): 13-22.

[5] LI Jing, WEN Guoyi, YANG Xiaofei, LI Xiuren. Mechanism of ocean carbon sink and development measures[A]. Ocean development and management, 2018.